Biomass Conversion and Biorefinery (2024) 14:5803–5818
https://doi.org/10.1007/s13399-020-00946-0

ORIGINAL ARTICLE

Assessment of hydro-mechanical properties of biochar-amended soil sourced from two contrasting feedstock

Sanandam Bordoloi[1,2] · Himanshu Kumar[1] · Rojimul Hussain[2] · Ravi Karangat[2] · Peng Lin[3] · Sekharan Sreedeep[2] · Hong-Hu Zhu[4]

Received: 14 May 2020 / Revised: 27 July 2020 / Accepted: 4 August 2020 / Published online: 9 August 2020

Abstract

In geo-environmental applications, the potential of biochar has been explored as a suitable cover material of landfill and vegetated slopes. The inherent nature of biochar affects the geo-environmental properties of the soil-biochar composite like water retention, compressive strength, infiltration, and soil erosion. Performance of a cover depends on biochar's surface functional groups, which can be either hydrophobic or hydrophilic based on bio-source. The objective of this paper is to investigate the geotechnical properties of biochar-amended soil sourced from two contrasting feedstock, i.e., poultry litter (animal based) and water hyacinth (plant based). The test results show that biochar addition increased the Atterberg limits and reduced the acidity of soil. Biochar addition directly increased the optimum moisture content and decreased the maximum dry density. Both biochar addition decreased the composite compressive strength by 25–50% but increased the ductility of composite. Water hyacinth biochar (WHB) inclusion decreased the erosion rate of soil while it is not the same for poultry litter biochar (PLB). In the case of water retention, only the addition of WHB increases retention and holding capacity of soil. The obtained results have been discussed in context with the conducted microstructural, chemical, and physical tests on both biochar. Through these analyses on biochar of different origin and having contrasting functional groups and intra-pore network, the development of a complex biochar-water network was confirmed.

Keywords Biochar · Geotechnical properties · Hydrophilic · Surface functional groups

1 Introduction

Biochar, a carbon-rich porous material, has been extensively used as soil amendment material to promote vegetation growth for potential applications such as ecological restoration, landfill cover, bio-engineered slope, and green roof (Fig. 1) [1–3]. Biochar is the carbonaceous residue left after pyrolysis process, which is characterized by thermal degradation of organic biomass in the absence or limited supply of oxygen [4]. During pyrolysis, as temperature increases, the organic material gradually turns in to char with gradual formation of aromatic sheets, higher surface area, and porosity

✉ Hong-Hu Zhu
zhh@nju.edu.cn

Sanandam Bordoloi
sanandam@ust.hk

Himanshu Kumar
hkumar@connect.ust.hk

Rojimul Hussain
rojmul.hussain@iitg.ac.in

Ravi Karangat
ravi.civil@iitg.ac.in

Peng Lin
plin@stu.edu.cn

Sekharan Sreedeep
srees@iitg.ac.in

[1] Department of Civil and Environmental Engineering, Hong Kong University of Science and Technology, Hong Kong, SAR, China

[2] Department of Civil Engineering, Indian Institute of Technology Guwahati, Guwahati, India

[3] Department of Civil and Environmental Engineering, Shantou University, Shantou, China

[4] School of Earth Sciences and Engineering, Nanjing University, Nanjing, China

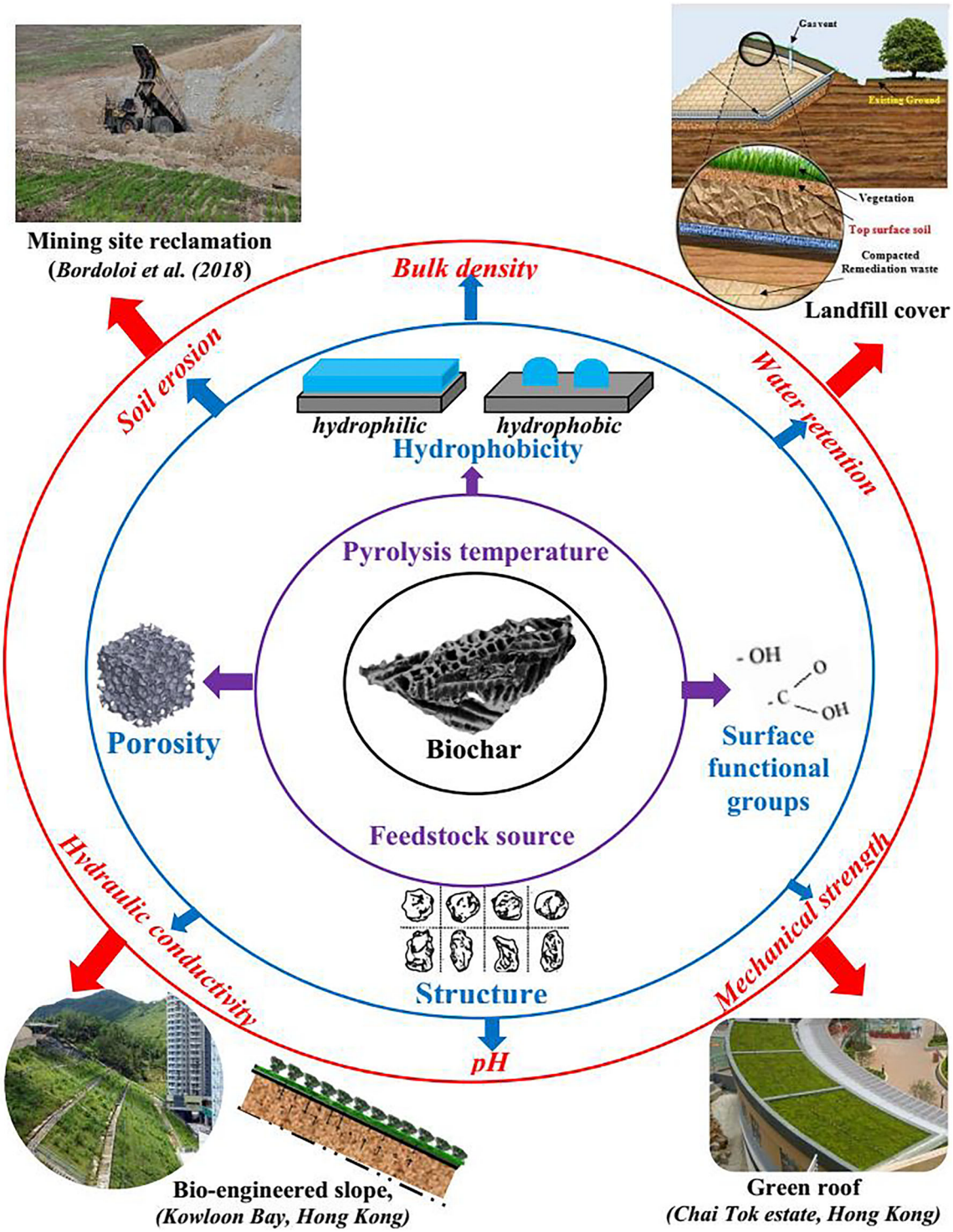

Fig. 1 Schematic description of the concentric circles showing the effect of biochar production (purple) on inherent biochar properties (blue) and geotechnical properties of biochar amended soil (red)

[5]. Biochar when mixed in soil modifies the pore size distribution of soil, provides additional nutrients for plant roots, and generally increase the soil water retention capacity [6]**.** The feedstock used for biochar are majorly organic waste biomass (both plant and animal based) [7]. Their (animal and plant-based feedstock) response to thermal degradation is different due to their inherent biopolymers [8, 9]. Animal biopolymers mostly constitute of animal protein such as gelatin, collagen, and polysaccharides like cellulose, starch, carbohydrates, etc. On the other hand, plant biopolymers are mostly lingo-cellulosic in nature, i.e., they are majorly constituted by cellulose, hemicellulose, and lignin; and have a defined structure

[10]. Conversion of waste biomass to biochar enhance the stability of the carbon and assists in long-term carbon sequestration [11]. Biochar has found popularity in agricultural applications and forest ecology as a soil medium, suitable for microbial incubation and water retention [6].

In geotechnical and geological applications, the potential of biochar was explored as a suitable cover material in landfill applications [12–16] and vegetated slope stability [17, 18]. These works in landfill applications majorly encapsulate the response of biochar amendment to methane gas transport, adsorption, oxidation, microbial activity, water holding capacity, and hydraulic conductivity [19–23]. Sadasivam and Reddy [24] have investigated the shear parameters of soil-biochar composite for landfill conditions and indicated that biochar addition can increase the stability of the cover system. Yargicoglu et al. [25] characterized the physio-chemical properties of different plant-based biochar but not the soil-biochar, composite. The vegetation potential in compacted biochar amended soil was also explored with respect to soil water retention characteristics (SWRC) and vegetation growth [10, 17, 26, 27]. In all of these geotechnical studies involving compacted soil-biochar composite, only plant-based commercial biochar was utilized and rarely any considerations were given to the aromaticity of the biochar in form of surface functional groups. This directly will affect geo-environmental properties like SWRC, cohesive strength, water flow, and soil erosion [28–30]. Pardo et al. [31] recently explored the impact of surface functional groups and inherent porous morphology toward liquefaction potential of sand. It is thus important to properly investigate the biochar type (based on plant or animal source) in form of surface functional groups, inherent morphology, and utilize it for geotechnical applications like slope protection.

The overarching objective of this note is to explore the influence of animal and plant-based biochar on geotechnical properties of soil. These are initial tests to comprehend the feasibility of biochar produced from contrasting feedstock. This was initially done by producing two different in-house biochar (plant and animal) based on its thermal degradation response. Thereafter, surface functional groups, surface morphology, and allied physio-chemical properties were characterized. Subsequently, the effect of biochar inclusion in altering the basic geotechnical properties of soil, at different weight percentage (5% and 10%) of dry soil was investigated. Based on the individual compaction characteristics of the soil and soil-biochar composite, the compressive strength, erosion potential, SWRC, and infiltration rate were assessed for the same compaction conditions. The study aims to highlight the underlying mechanism of soil-biochar composite in terms of mechanical and hydraulic response, and juxtapose it with inherent functional groups and morphology of the biochar.

2 Experimental plan and procedure

The general schematics of experimental plan and procedure was described in Fig. 2. The pyrolysis condition was determined based on thermogravimetric analysis (TGA) of the selected feedstock. The produced biochar was investigated for elemental composition, surface morphology, and surface functional groups. The soil-biochar composite with biochar at 5% and 10% of dry soil was investigated thereafter for basic geotechnical properties such as grain size distribution, Atterberg limits, compaction characteristics, shrinkage area ratio, and pH. Based on the obtained compaction characteristics of individual composite and BS, samples were compacted at the same compaction state. The compaction state was selected at 90% of maximum dry density (MDD) and corresponding optimum moisture content (OMC) along the compaction curve. This is done as biochar in geo-environmental applications are predominantly used for vegetative covers and vegetation growth is suitable up to around 0.9 MDD [32]. To account for its feasibility in geo-environmental application, a series of mechanical and hydraulic tests were done on the compacted sample whose details are given below. Each experiment was repeated thrice for accuracy and standard error was reported.

The mechanical tests done were unconfined compressive strength (UCS) test [33] and pin-hole test [34] to measure quantitative compressive strength and erosion potential, respectively. The hydraulic assessment was done by measuring the soil water retention property and infiltration rate by conducting instrumented column test [35] and disk infiltration test [36], respectively. The UCS test setup is shown in Fig. 3a and the strain rate selected for shearing was selected at 1.25 mm/min. The schematic steps of pin hole test setup are shown in Fig. 3d. The samples were compacted using a static compactor from both sides and a hole of 0.7 cm was drilled into the compacted sample. The runoff flow rate was initiated from 0 to 1 l/min and runoff can pass through the compacted sample for 10 min [37]. The effluent water is collected in a chamber after it passes through the sample and later filtrated using a Whitman 42 grade filter paper. The soil loss is thus calculated from the retained soil mass on the filter paper. Pinhole is a popular index test to measure internal erosion of a soil or soil composite [38, 39]. The use of pin hole erosion setup is limited to investigate piping or internal erosion. Erosion due to surface runoff cannot be calculated using pin hole erosion setup.

The soil water retention characteristics (SWRC, i.e., matric suction vs. moisture content) is measured by an instrumented column setup as shown in Fig. 3b. The experiment was conducted under a controlled environment (temperature and relative humidity, RH) to minimize the variability associated with SWRC. The temperature and RH were kept at 24 °C and 40% respectively. Dummy sensors were pre-installed during

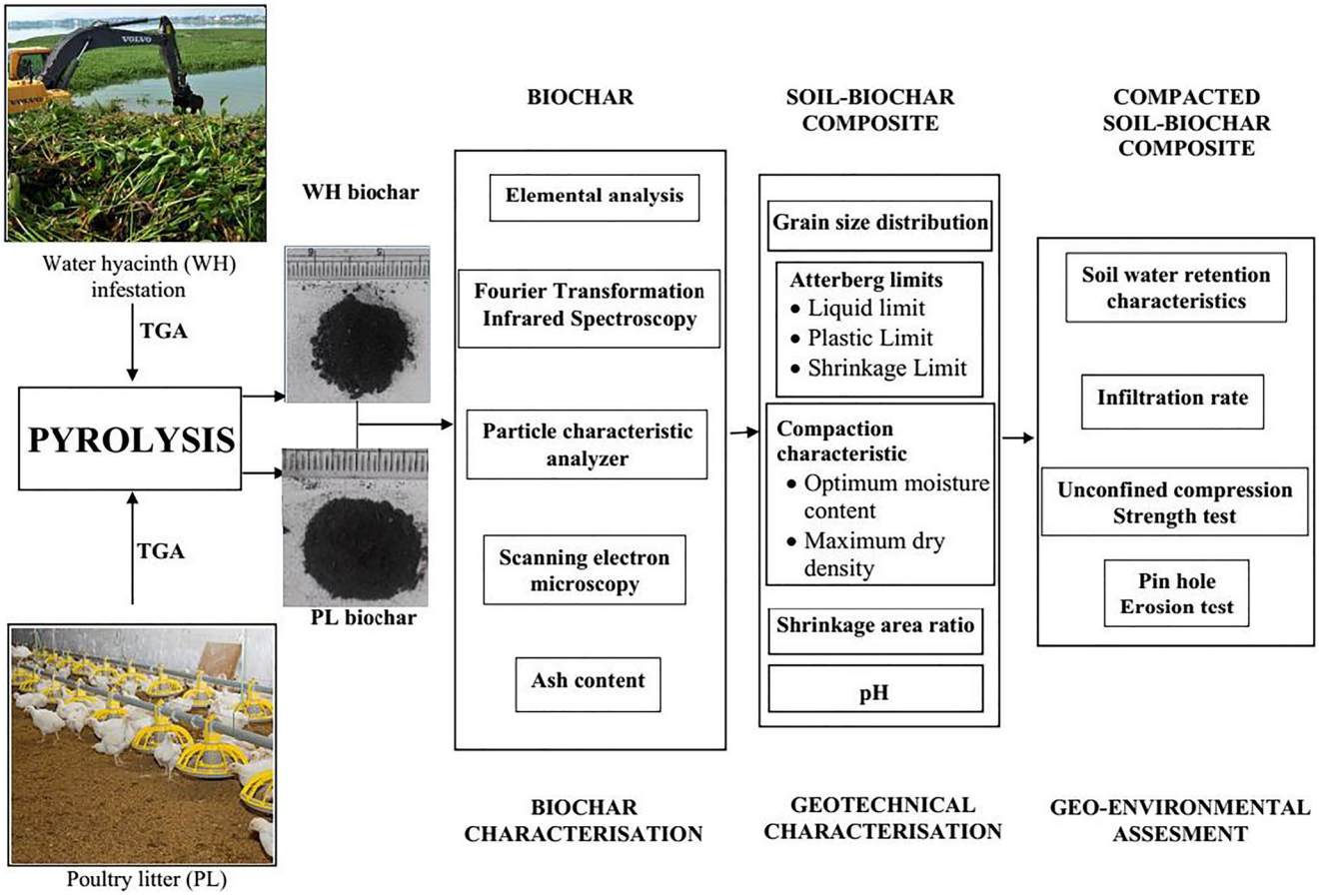

Fig. 2 Flowchart of the experimental program in this study

compaction process so that there is no damage to the ceramic sensors. Thereafter, the sensors are installed carefully so that there is proper contact between sensor and soil. The column dimension and sensors were installed at location as per previous literature pertaining to SWRC measurement [10] and shown in Fig. 3b. Decagon's MPS-6 suction sensors and EC-5 moisture sensors were used to measure the matric suction and volumetric water content respectively [35]. Decagon's EM-50 data logger system was used to store the data of the two sensors. The van Genuchten fitting [40] was not done to the measured data points of the SWRC as the residual water content of individual soil-biochar composite is not known because MPS-6 only measures suction accurately up to 2000 kPa [35].

The surface infiltration was measured using Decagon's mini disk infiltrometer (MDI) by conducting infiltration tests on column setups. The column dimension was chosen to avoid any boundary effect as per previous literature [41]. Three repetitions were done for each experiment conditions. The tension applied to all experiments were corresponding to 2 cm head and a minimum amount (15 mL) of water could infiltrate in the soil as per literature [42]. MDI was chosen to conduct infiltration experiments as it is easy to use in laboratory settings and there is no need of auguring. A simplified approach of measuring infiltration rate was adopted as per literature [36]. Infiltration rate (I) at any time interval (dt) was determined in Eq. 1

$$I(t) = \frac{1}{A}\left(\frac{\mathrm{d}V}{\mathrm{d}t}\right) \tag{1}$$

where dV is the volume change of infiltrated water within a given time (dt) and A is the cross-sectional area of the disk.

3 Materials

3.1 Soil characterization

The soil used in the current study was classified as silty sand (SM) as per the unified soil classification system (USCS; [43]). As per ASTM D4318-10 [44], the liquid, plastic, and shrinkage limits of the soil were 36%, 25%, and 14%, respectively. The grain size distribution of the soil was presented in Table 1 as per ASTM-D422–63-07 [45]. The specific gravity of the soil is 2.58 as per ASTM-

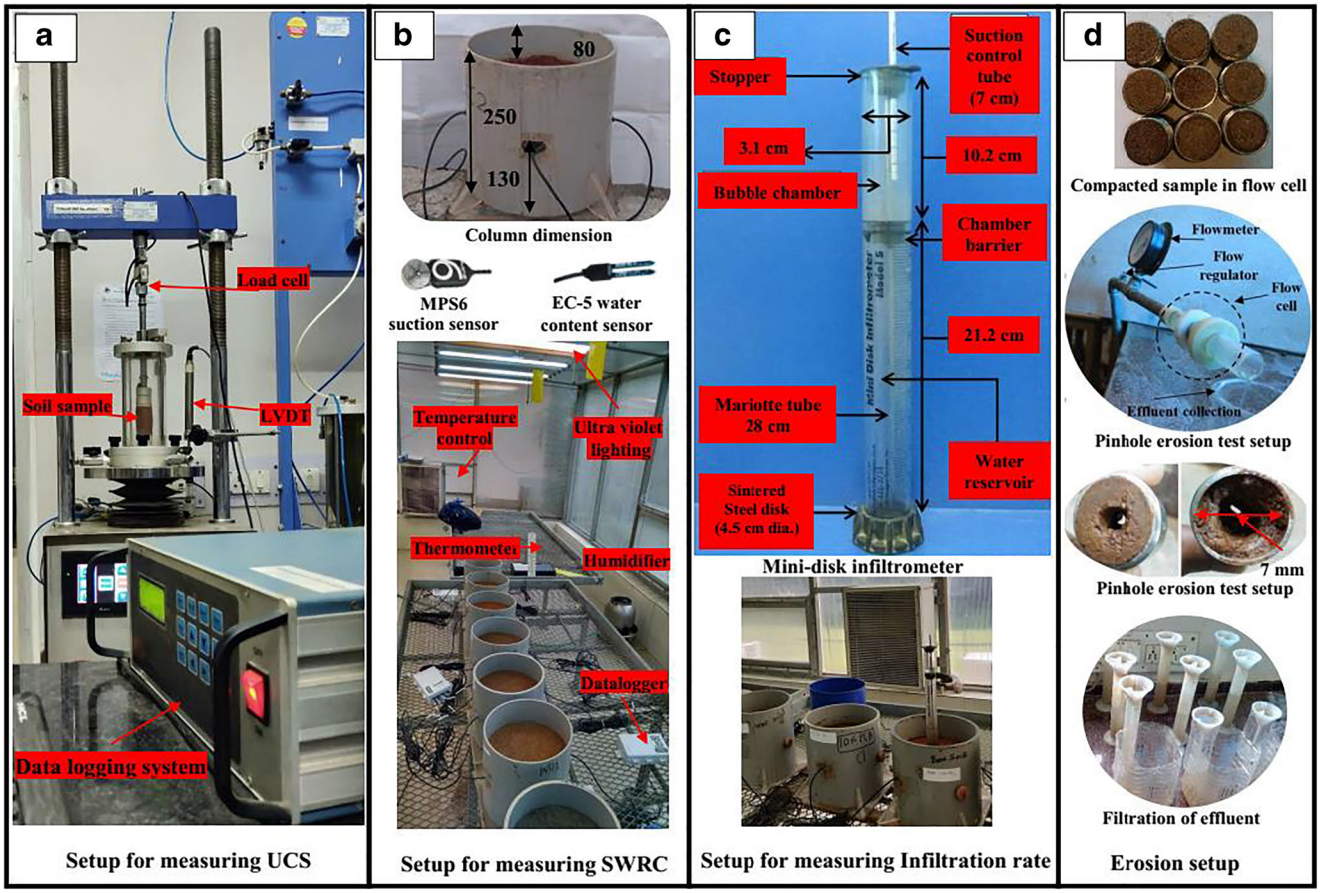

Fig. 3 Photographs of the experimental setup used to measure (a) UCS, (b) SWRC, (c) Infiltration rate, and (d) Soil erosion rate

D854 [46]. The compaction characteristic (i.e., maximum dry density and optimum moisture content) for the soil are 1.7 g/cm^3 and 16.7% respectively [47].

3.2 Biochar production and characterization

Two biochar (produced from water hyacinth (WH) and poultry litter (PL)) were selected to investigate the effect of plant and animal-based biochar. The WH plants were selected from the same water body to minimize the effect of any genetic variation. The poultry litter was sourced from a local chicken farm. The TGA was initially done on both biochar to decide the pyrolysis temperature of the feedstock. As per the TGA curve and mass loss observed of the feedstock (Fig. 4a), pyrolysis temperature in the pyrolizer was chosen at 390 °C and 450 °C for WH and PL (Table 2). Slow pyrolysis was chosen as the pyrolysis method for biochar production as it offers the highest yield of biochar [48]. Fourier transform infrared FTIR spectrometer was consequently used to investigate the surface-active functional groups of the two produced biochar [49]. FTIR methodology consists of passing infrared days through the biochar sample. Based on the functional groups present in the biochar surface, some wavelengths will be absorbed and the rest will be transmitted. The spectrum obtained (Fig. 4b) of transmittance (in this case) or radiance along with the wave number gives the qualitative surface functional groups. In the case of WH, the predominant surface functional group is hydrophilic hydroxyl (OH) group with neutral ether (C-O) being the second group [50]. The poultry litter biochar (PLB) had predominantly hydroxyl group (OH) with significant peak stretching. In contrast to water hyacinth biochar (WHB), there were additional hydrophobic functional groups like alkyl aliphatic (CH) group as well as aromatic hydrophobic groups such as (C-C) and (C-OH) present in PLB [51]. Elemental analysis of C, H, N was done using an

Table 1 Particle size distribution of the soil and the selected biochar

Group	Bare soil	WHB	PLB
Gravel (> 4.75 mm)	0	0	0
Coarse sand (2.00–4.75 mm)	4	0	0
Medium sand (0.425–2.00 mm)	24	32	32
Fine sand (0.075–0.425 mm)	23	40	52
Silt (0.002–0.075 mm)	34	28	16
Clay (< 0.002 mm)	16		

Finer percentage for biochar could not be ascertained by conventional method

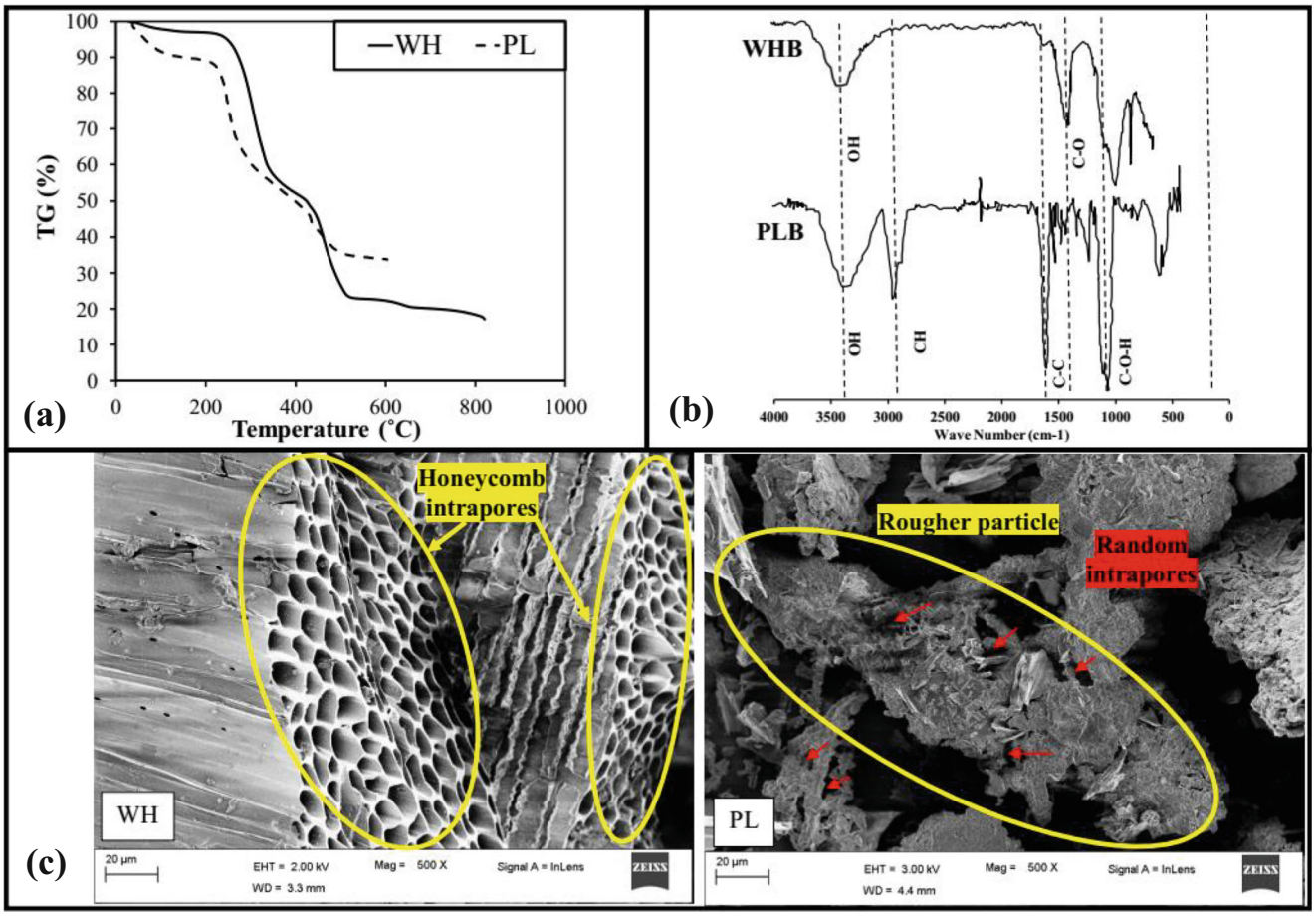

Fig. 4 Biochar characterization through **a** TGA analysis of feedstock, **b** FTIR, and **c** FESEM analysis at × 500 magnification

elemental analyzer and reported in Table 2. The percentage ash content and cation exchange capacity (CEC) was measured by [52, 53], respectively.

Field-emission scanning electron microscopy (FE-SEM) imaging was conducted to observe the surface morphology of the two biochar (Fig. 4c). Both materials showcase some porous nature on the surface at same magnification (× 500). However, WH had clear honeycomb porous surface indicating high amount of intra-pores. This honeycomb structure of intra-pores in the case of plant-based biochar was due to lignin biopolymer encapsulating cellulose and hemicellulose biopolymers [54]. During pyrolysis, the hemicellulose and

Table 2 Production conditions, elemental composition, and other chemical properties

	WHB	PLB
Feedstock	Water hyacinth stem sourced from deepor lake, India	Straw, chicken feces, bentonite clay (2%), basal dust (~ 1%) and traces of FeO_2
Pyrolysis process	Slow pyrolysis	Slow pyrolysis
Pyrolysis temperature (°C)	350–400	450
Elemental analysis		
C (%)	53.39	36.41
O (%)	42.80	61.73
H (%)	1.99	1.86
N (%)	1.82	2.39
Ash content (%)	39	56
CEC (cmol kg^{-1})	21.95	56.3

cellulose degrades first, and lignin degrades last. This thermal degradation leads to honeycomb intra-pores which can facilitate water within the pores [31]. In the case of PLB, these stacked honeycomb pores are not found. Rather, the pores are random in nature and smaller in number. These can be due to the absence of a lignocellulose arrangement of biopolymers found in plant-based material. Moreover, the FE-SEM analysis showcased that PLB particles have a comparatively rougher surface as compared to WH.

The particle surface morphology was further investigated by Occhio 500nanoXY particle shape and size analyzer [55] used for precision measurement of powdered materials (see Fig. 5a). The instrument consists of an integrated computer with an in-built imaging software and a particle dispersion device that facilitates capturing of powdered material (Fig. 5a, b). The software can measure particle and its morphology ranging from 0.2 to 2000 μm [56, 57]. The shape parameters obtained, and their definition have been reported in Table 3. However, three major parameters, i.e., roundness (Waddel's concept in Fig. 5c), circularity, and Occhio roughness was discussed majorly to explain the mechanical parameters tested in results section. PLB has a rougher surface and low roundness which can facilitate greater soil-biochar and biochar-biochar interface friction as compared to WHB.

4 Results and discussion

4.1 Atterberg limits, shrinkage area ratio, and pH of soil-biochar composite

Figure 6a, b showcases the liquid and plastic limit respectively for the two biochar. It was seen that soil-biochar composite showed significant increase (6% to 14% for WH) in liquid limit proportional with the amendment percentage. The inclusion of PLB to soil increases the liquid limit by 3% to 8% for 5% and 10% biochar amendment, respectively. The higher liquid limit in soil-biochar composite was attributed to the presence of intra-pores within biochar particle (Fig. 4c) increasing the composite porosity [17]. The intra-pores increase specific surface area (SSA) of the biochar [58] facilitating more water within the soil-biochar composite. The plastic limit for WHB-soil composite also showed similar increase (4% to 16%) with respect to bare soil. In the case of PLB-soil composite, there was rarely any change in the plastic limit and can be attributed to less number of intra-pores in biochar particle (refer Fig. 4c). Reddy et al. [12] have also reported an increase in liquid and plastic limit based on a plant biochar (species not mentioned) at 5%, 10%, and 20%.

The shrinkage limit for soil-biochar composite decreased by (2–3.5) % from bare soil for both biochar types as shown in Fig. 6c. To further comprehend the shrinkage potential of the

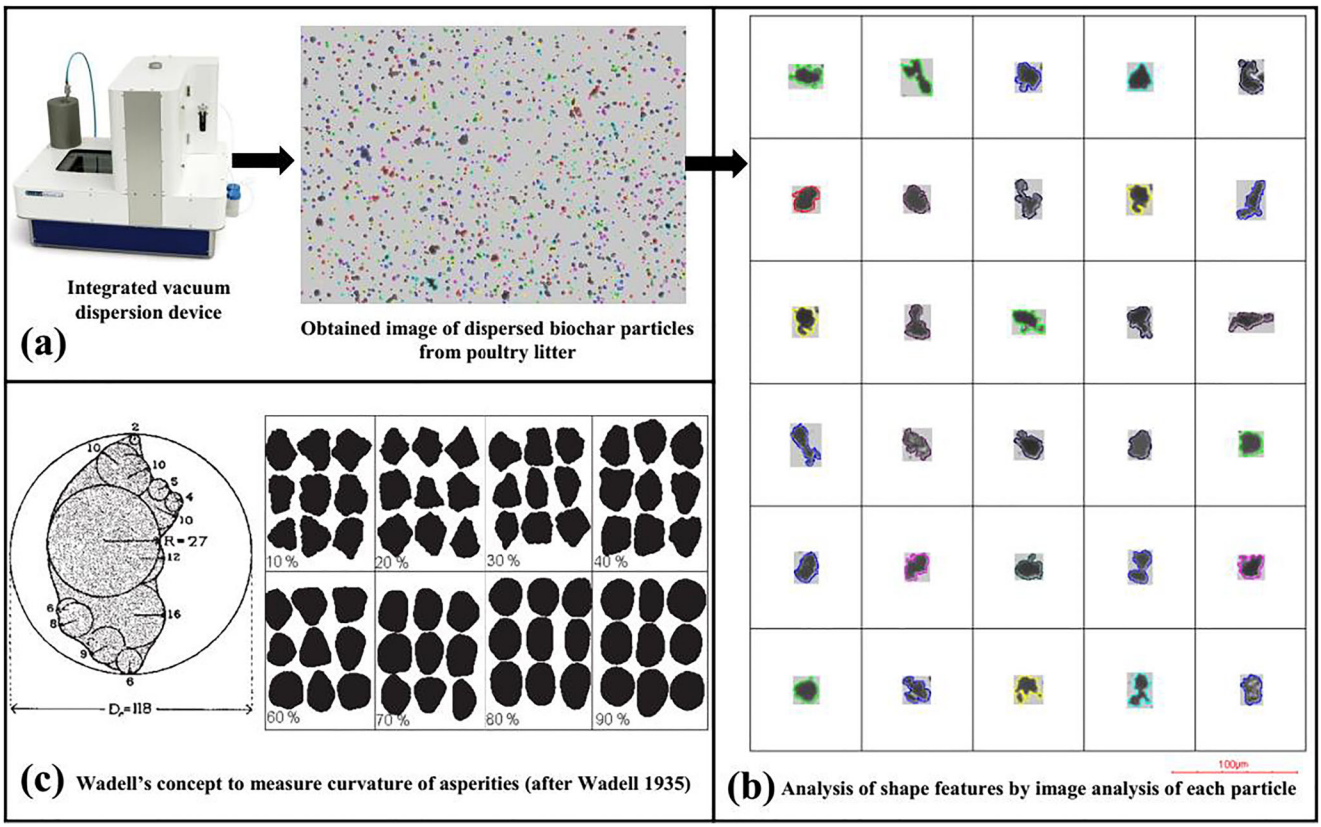

Fig. 5 Description of **a** the 500nano XY particle shape analyzer, **b** the resultant images of biochar, and **c** the concept of particle roundness (after [52])

Table 3 Mean shape parameters measured from particle characteristic analyzer

Parameter	Definition	Mean value	
		PLB	WHB
Volume-equivalent diameter (μm)	The diameter of a sphere having the same volume as the particle	9.0	3.8
Area-equivalent diameter (μm)	The diameter of a sphere having the same projection area as particle	10.6	8.6
Inner diameter (μm)	The biggest circle inscribed into the projection area of the particle.	7.4	7.1
Thickness (μm)	Approximation of the particle width for very long and concave particle	3.9	4.3
Roundness (%)	The degree to which the projection area of the particle is similar to a circle. The ration of the area-equivalent diameter to Feret diameter maximum	58.4	76.4
Circularity (%)	The degree to which the projection area of the particle is similar to a circle, considering the smoothness of the perimeter.	74.7	83.6
Occhio roughness 80% (%)	The ratio of smooth reference to the particle projection area. The smooth reference is defined by inscribed circles tangent to each point of the particle projection outline with a radius greater than 80% of the maximum inscribed circle	24.5	14.8

composite, the shrinkage area ratio (SAR) was measured (Fig. 6d). SAR is ratio of change in area of sample after drying to initial area of sample. The initial sample was in slurry form mixed at liquid limit and kept in shrinkage disk. All samples were dried at 80 °C in an oven for 24 h and measurement was done based by image analysis technique. It was seen that soil-biochar composite decreased the shrinkage area ratio of bare soil by around 10–11% due to the non-cohesive nature of biochar [12, 59].

Alkalinity or pH of a soil have cascading impacts on numerous processes which are important for top layer functioning of landfill systems such as methanotrophic activity, mineral precipitation, and greenhouse gas emissions [60, 61]. Figure 7 shows the effect of biochar addition on soil. Each

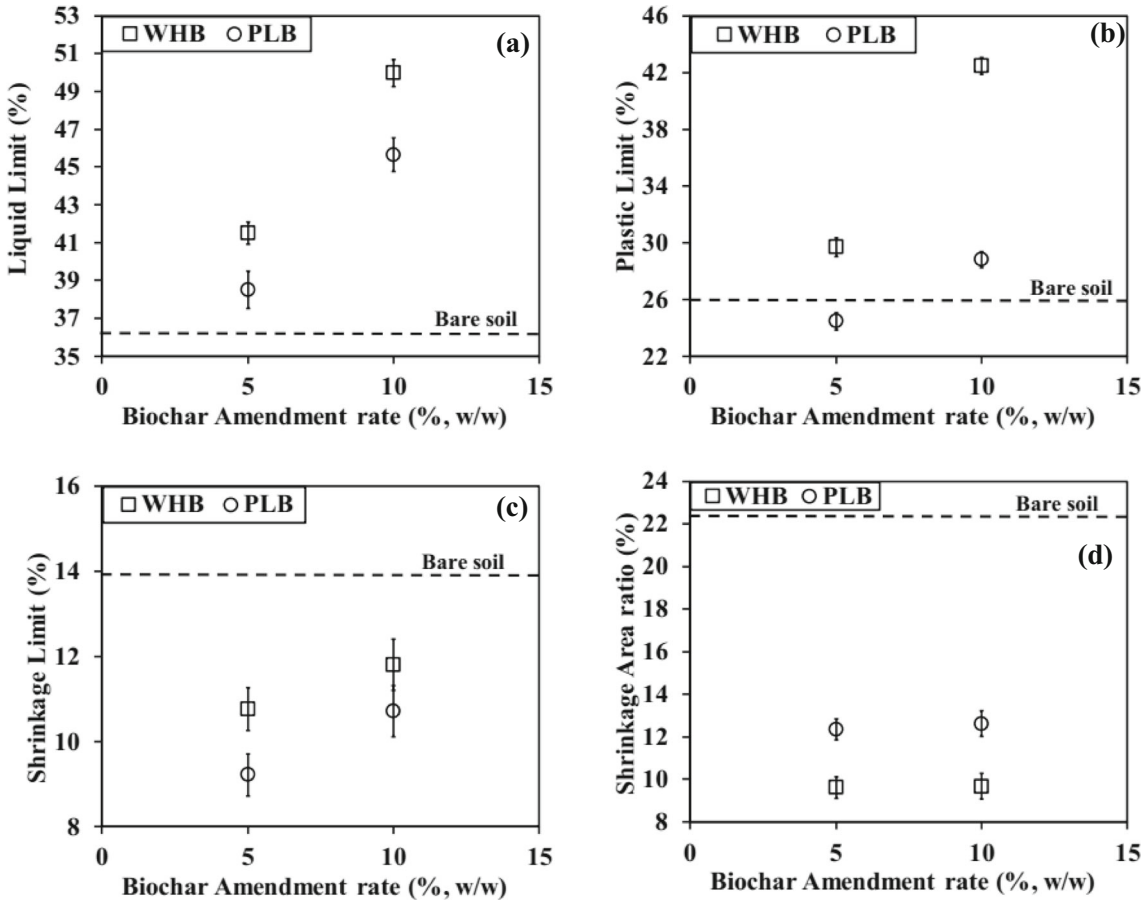

Fig. 6 **a**–**c** Atterberg limits and **d** shrinkage area ratio of the soil-biochar composite

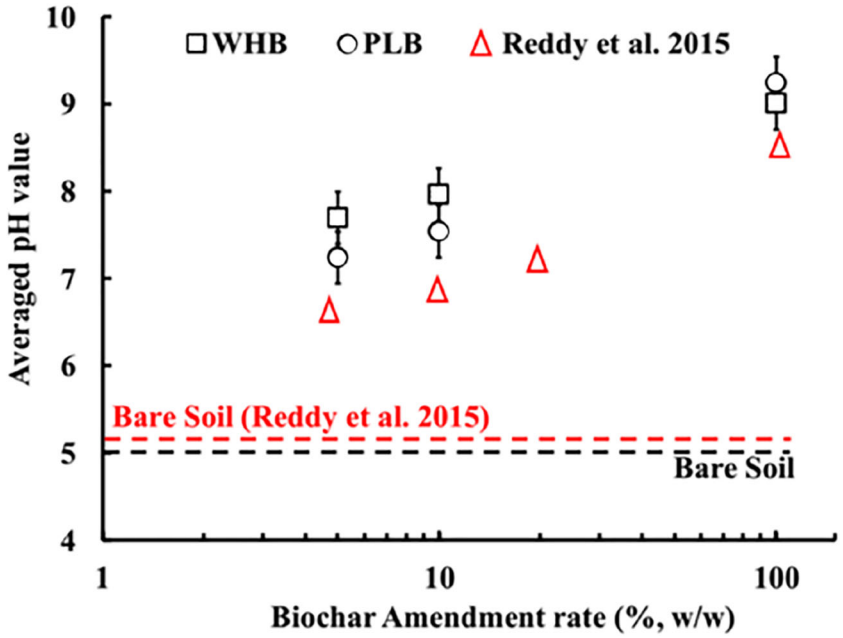

Fig. 7 Effect of biochar amendment on pH of the soil-biochar composite

biochar was basic in nature (9.2–9.4) and upon addition to acidic soil (i.e., bare soil) resulted in soil being relatively neutral or slightly basic (7–8). Similar response was found in a study conducted by Reddy et al. [62] where pH levels of 6 to 8 was found to be optimal for methanotrophic activity [63]. Literature attributes the alkalinity of the biochar due to surface functional groups such as carbonates, hydroxides, and other inorganic alkalis which was reflected in the FTIR response of both biochar [64].

4.2 Compaction characteristics of soil-biochar composite

Figure 8 describes the compaction curves for soils and soil-biochar composite as per standard proctor test. The MDD and corresponding OMC for the bare soil were 1.69 g/cm^3 and 17% respectively. The biochar-amended soil showcased a decrease of MDD while OMC increased with addition of biochar from 5 to 10%. The decreased MDD can be explained by the lower specific gravity of biochar particles and the smaller compressibility of the amended soils at a given compaction energy [62, 65]. The higher optimum water content could be caused by the porous morphology (Fig. 4c) and high surface area of biochar particles [66]. Figure 8c shows the schematic representation of how the morphology changes with inclusion of biochar and how excess water can be stored with the biochar particle matrix [67]. Ni et al. [17] also observed for silty sand soil that 10% of peanut shell biochar addition also decreased MDD from 1.89 to 1.74 g/cm^3. OMC increase by 5% corroborates the current finding of OMC increase of 4% in the case of plant-based biochar. In the case of PLB, although there is shift in OMC by 2%, it is much less than the plant-based biochar possibly due to lower intra-pores.

4.3 Compacted soil-biochar composite

It is to be noted that all soils were compacted at 0.9 of maximum dry density and OMC for individual soil type to test the sample at equal compaction energy given to the soil. The compaction state was chosen based on the density required for vegetation growth [32]. The detailed discussion of the tests was done by explaining the mechanical properties (encapsulating UCS and pin-hole erosion test) followed by the hydraulic properties (water retention and infiltration).

4.3.1 Mechanical response of soil-biochar composite

Figure 9a represents the stress-strain response of individual sample for soil and compacted soil-biochar composite at 5% biochar amendment. It is seen that for addition of WHB and at 10% PLB, UCS decreases with respect to bare soil. Soil with 5% PL biochar addition resulted in a marginal increase of UCS (20–30) kPa (Fig. 9b). The lower UCS value for biochar-amended soils could be mainly attributed to the modification of soil porosity [59] due to intra-pores present in biochar. Sun and Lu [68] reported that biochar addition resulted in an increase of pore volume which will decrease the strength of the soil. Previous work done on direct shear by Sadasivam and Reddy [24] reported that hardwood biochar addition resulted in increase in cohesive strength and angle of friction. On the contrary, Zong et al. [59] reported that cohesive strength decreases from 25 to 60% by conducting

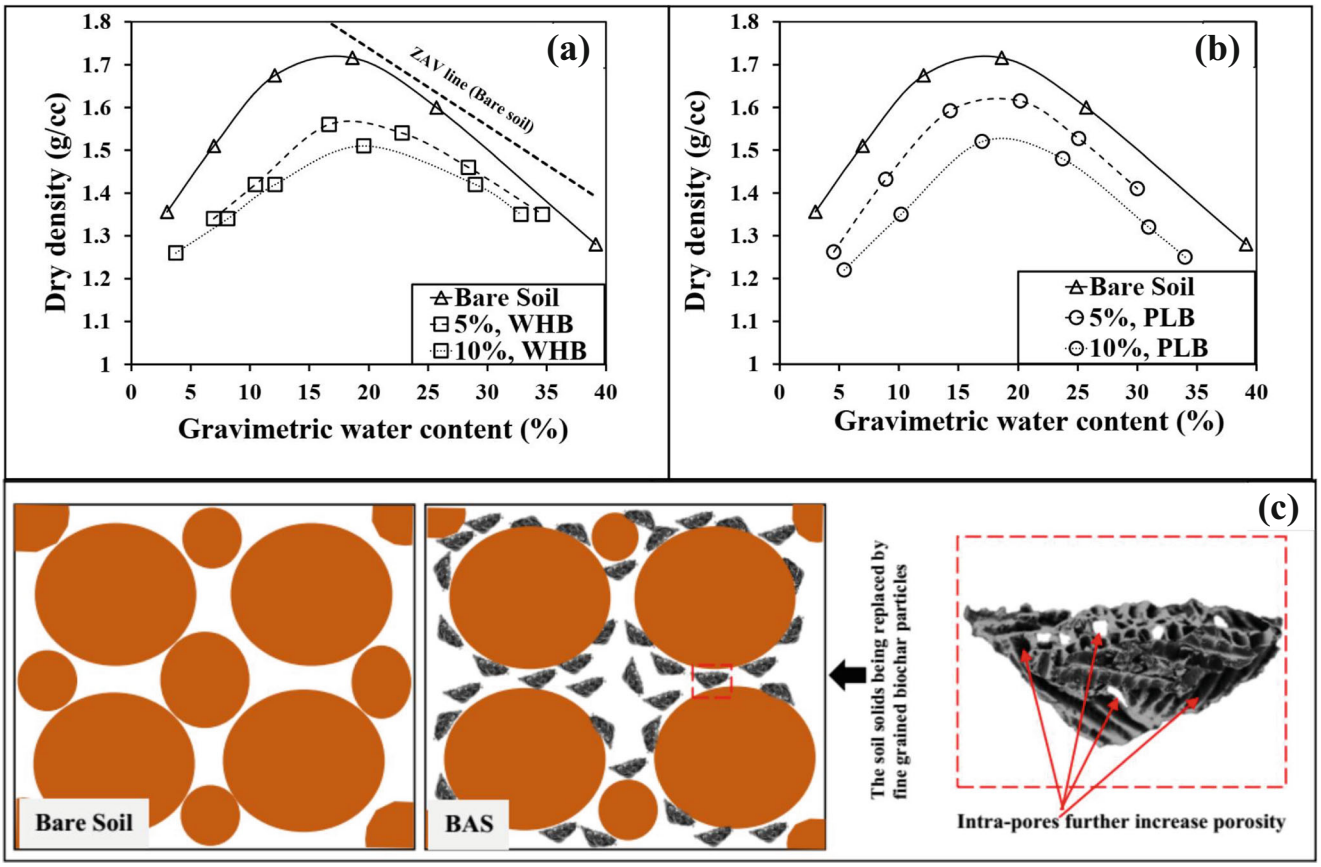

Fig. 8 Compaction curve of **a** WHB and **b** PLB to estimate the maximum dry density and optimum moisture content. **c** Schematic description of the change in particle matrix arrangement of soil due to biochar addition (after [52])

direct shear tests using three biochar (wheat straw, woodchips, and wastewater sludge).

The soil-biochar composite strength is partially determined by the frictional forces of soil-biochar interface. The strength of composite from WHB is way less as compared to PLB as the roughness of PL is much more (24.5%) than that of WH (14.8%) as showcased by particle characteristics analysis (Table 3). The failure patterns and post peak ductility of each soil type was found to be different. For simplicity, only 5% biochar-amended soil (Fig. 9a) is used to describe the post peak ductility using normalized ductility index, (NDI). NDI is defined as the ratio of fall in post peak strength to that of the peak stress [69]. Here, complete brittle failure (where σ_{ultr} or σ_{ultb} is taken as 0 at same strain) is indicated by NDI = 1. Contrastingly, purely ductile behavior with no change in stress on further straining (peak and ultimate values are same) is seen in the case of NDI being 0.

$$\mathrm{NDI} = \frac{(\sigma_{pr} - \sigma_{ultr})}{(\sigma_{pr})} \text{ or } \frac{(\sigma_{pb} - \sigma_{ultb})}{(\sigma_{pb})} \quad (2)$$

where σ_{ultr} and σ_{ultb} are the ultimate stresses for reinforced and bare soil, respectively. It was found that bare soil showcased distinct shear failure with relatively brittle failure having NDI between 0.67 and 0.7. Five percent PLB amended soil showed NDI value between 0.13 and 0.14 which indicates that the sample is relatively ductile. However, 5% WHB amended soil showed highest ductility (0.09 to 0.1) with multiple shear planes and bulging failure as shown in Fig. 9a.

The effect of biochar amendment on soil erosion was showcased in Fig. 10 based on pin-hole erosion test. Inclusion of WH biochar in soil decreases the erosion rate of soil after 0.5 Pa shear stress. This can be attributed to the abundant presence of hydrophilic functional groups which attract water molecules and increase the inter-particle bonds [70]. Furthermore, the roundness of WH particles was found to be very high (76%) as per particle characteristic analyzer. Thus, the stress caused by the water flow over the rounded biochar particles would be relatively less as compared to PL which is relatively coarse (circularity = 58%). It was seen that with WHB addition to soil, the erosion rate gradually decreases. In the case of PLB-amended soils, at 5% PLB-amended soil, the erosion increases after 0.2 Pa. It can be attributed to hydrophobic functional groups and probably the biochar dust coated on soil particles will further decreases the apparent cohesive forces between the soil [31, 59]. However, for 10% PLB, there is decrease in erosion rate which needs to

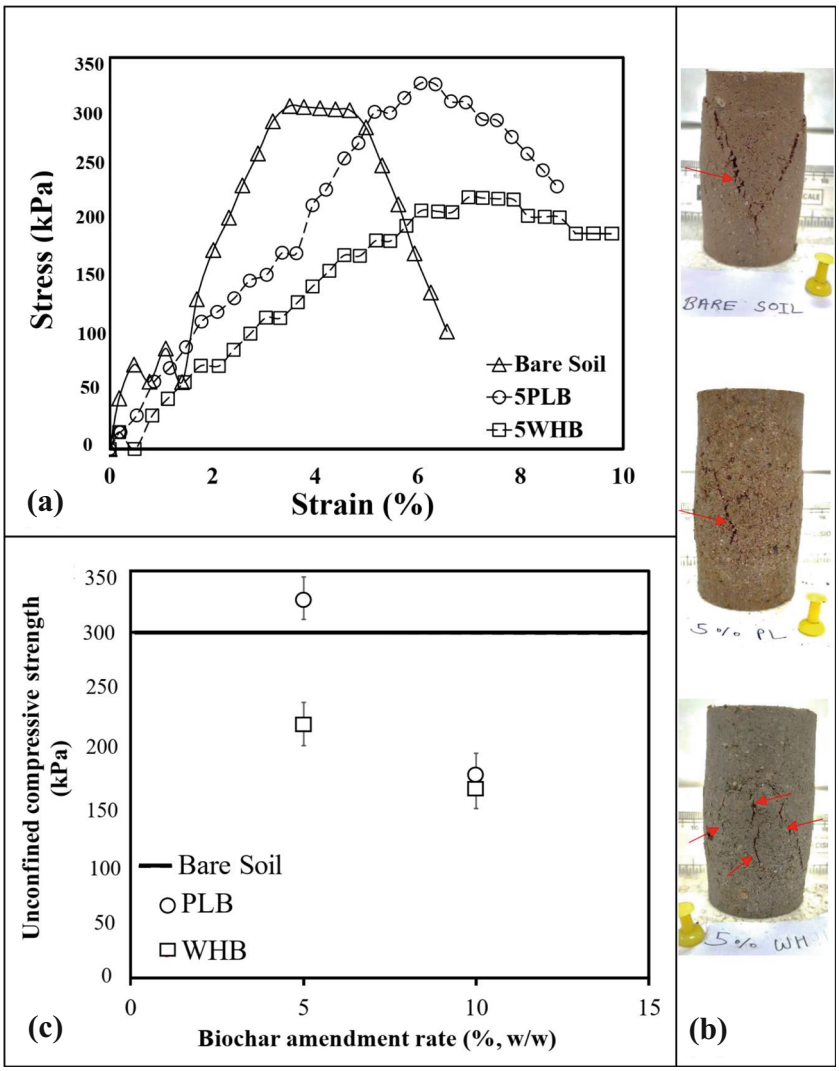

Fig. 9 Unconfined compressive strength of bare soil and soil biochar composite discussed in **a** general stress -strain response. **b** Sample at failure and **c** effect of percentage amendment

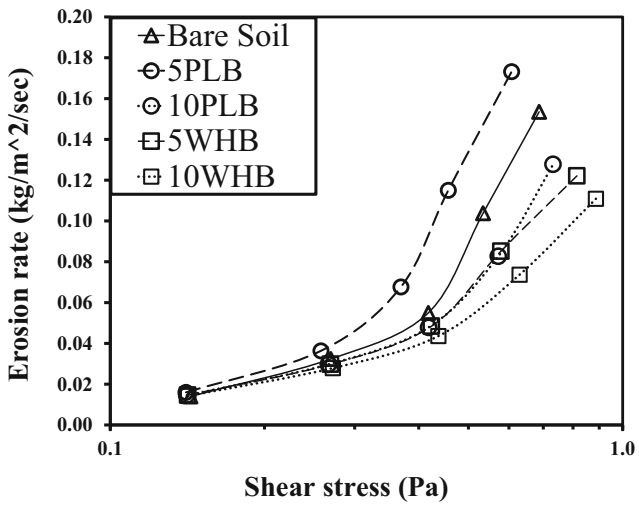

Fig. 10 Results of the pin-hole tests shown as soil erosion rate Vs shear stress and resultant average critical shear stress for bare soil and soil-biochar composite

be investigated in the future. Plausible reason may be that erosion rate is governed by both the functional groups (both hydrophilic and hydrophobic), surface roughness, as well as inter particle bonding due to rougher surface.

4.3.2 Hydraulic properties of soil-biochar composite

Soil water retention response of bare soil and soil biochar composite is shown in Fig. 11a based on the instrumented column setup. For 5% and 10% WHB-amended soil, at small suction range (< 100 kPa), retained water content increased by around 6% and 11% respectively as compared to bare soil. The increased magnitude is comparable with results by Ni et al. [17], who found that 10% biochar produced from plant-based peanut shell increased water content by 6–8% (from 1 to 10 kPa). Beyond 2 MPa (beyond wilting point), water content in 5% and 10% WHB-amended soil were higher by 5% and 11%, compared to

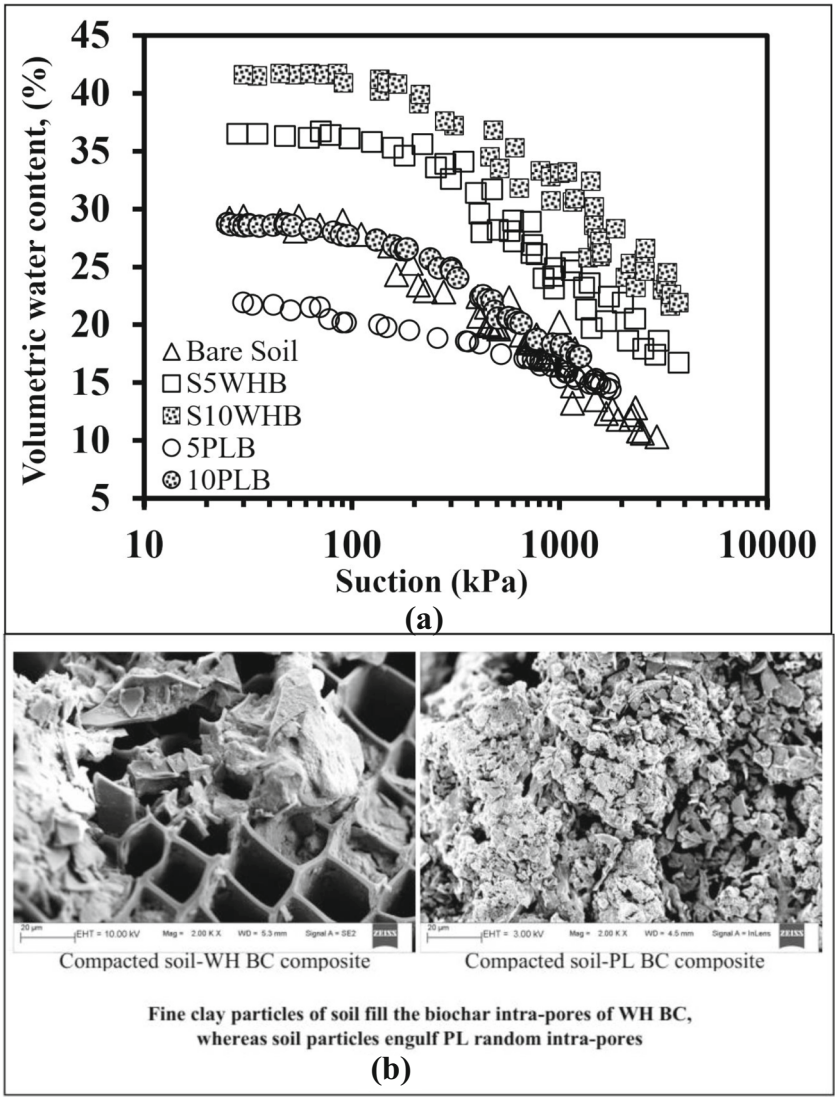

Fig. 11 **a** Soil water retention response of bare soil and soil biochar composites. **b** FE-SEM images of compacted soil-WHB composite and soil-PLB composite at 2KX magnification

that of bare soil. This indicates that WHB could retain soil water much more significantly at high suction ranges and is attributed to the intra-pores within biochar (Fig. 4c) and occupancy of inter-pore space by WHB particles. Moreover, the fine clay particles of soil could also fill the biochar intra-pores and thus decrease the pore diameter within biochar as hypothesized by T. F. Wong et al. [20] enabling more storage of water. This hypothesis was verified by taking FE-SEM images of compacted soil-biochar composites of both WH and PL feedstock (Fig. 11b). It is clearly seen that portion of clay and fine silt particles can fill the biochar intra-pores in case of WH, contrary to the case of PL where soil particles engulf the small sized and random intra-pores. The major surface functional groups (i.e., -OH, -CO) in the case of WH are hydrophilic. On the contrary, when biochar has hydrophobic functional groups such as PLB, biochar may have no effect on water retention of sandy soil as previously reported in literature [71]. This phenomenon is manifested for PLB-amended soil in the current study. There is a decrease in water retention for 5% PLB-amended soil in comparison to bare soil. On increasing the biochar amendment to 10%, the SWRC is almost identical to bare soil. There is obviously an effect of surface hydrophilic groups as well as relative less amount of intra-pores. Hydrophobic functional groups like alkyl (-CH) and aromatic groups (C-C and C-OH) repel water and thus may decrease the water retention capacity of soil-PLB composite.

Surface infiltration response of bare soil and soil biochar composite was shown by plotting the cumulative infiltration with time graph in Fig. 12a. It was observed that inclusion of biochar in the current soil reduced the infiltration rate regardless of being either plant or animal based. This was evident because of the fine-grained average diameter of the biochar (3.8–9 μm). Inclusion of biochar made the soil relatively fine grained (having smaller pore throat size, refer to Fig. 8c) and

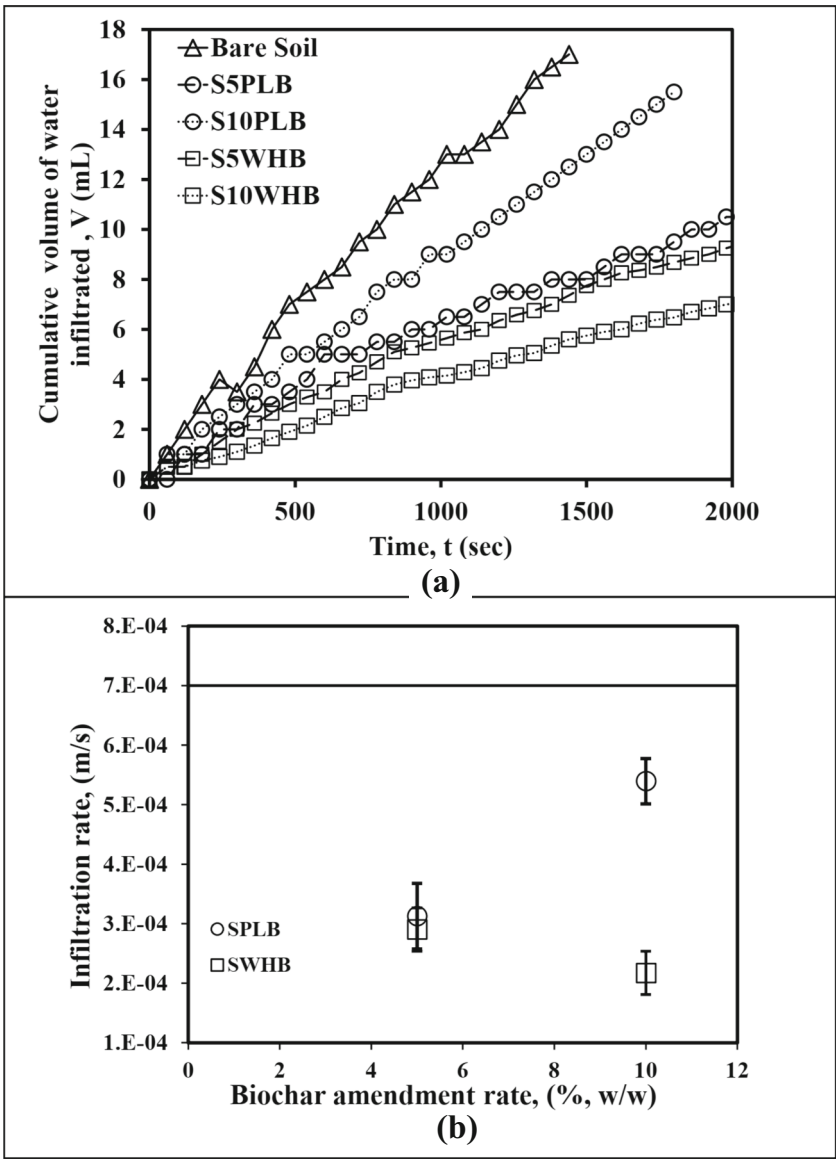

Fig. 12 Infiltration response of bare soil and soil biochar composite. **a** Infiltration vs time response, and **b** effect of percentage amendment

thus there is a decrease in infiltration rate in the same order (Fig. 12b). Furthermore, the tortuosity due to water flow along the biochar intra-pores might additionally hinder water transport along the soil-biochar composite. Among the two biochar, WH showcased lower infiltration rates as compared to PL possibly as it is finer in size (refer Table 3). SWCCs of bare soil and 10PLB show no significant differences and it is expected that their infiltration rate should be also relatively the same in magnitude. However, it is to be noted that infiltration rate of bare soil and 10PLB is in the same order (refer Fig. 12b), with only difference by a magnitude of 1.5. Also, the difference in magnitude of that small order can be brought out by change in contact angle [51] due to hydrophobicity of PLB, as indicated by the FTIR spectra. The effect of biochar percentage on infiltration rate did not give substantial trend and needs further investigation.

5 Concluding remarks

Two biochar (WHB and PLB) of contrasting plant and animal origin was produced using slow pyrolysis in an in-house pyrolysis system. Each biochar was characterized for elemental composition, surface functional groups, and morphology (using FE-SEM and particle characteristic analyzer). The biochar was mixed with a silty sand soil at 5% and 10% by dry weight of soil and initially characterized for basic geotechnical properties. The change in geotechnical properties for the individual soil-biochar composites were explained in conjuncture with biochar porosity (including inter and intra-pore arrangement) as well as by hydrophilic or hydrophobic surface functional groups. It was revealed that biochar addition can increase the Atterberg limits (except shrinkage limit) and reduce the acidity of soil for suitable plant growth conditions. Biochar

addition directly increased the optimum moisture content and decreases the maximum dry density of the soil.

The mechanical tests revealed that biochar addition in silty sand at same compaction energy decreased the composite compressive strength by 25–50%. This is more profound in the case of plant-based WHB addition to soil at any percentage reinforcement. It is only at 5% addition of PLB in soil that there is a meager increase (5%) in compressive strength and can be attributed to the rough morphology of biochar particle. However, for all biochar, the ductility of the composite increased manifold as indicated by higher NDI values. WHB decreases the erosion rate of soil due to its hydrophilic functional groups and rounded particles. However, for 5% PL, an increase in soil erosion was observed. In the case of water retention, the addition of plant-based WHB increased the water retention and holding capacity of soil. However, for PLB, a reduction in water retention is observed. The infiltration rate decreased for both soil-biochar composites as compared to bare soil. But the decrease is in the same order as that of bare soil. Through these analyses on biochar of different origin, the development of a complex biochar-water network was confirmed. Some results contrast with previous literature in geo-environmental application which has majorly focused on plant-based biochar. The study aims to draw attention to the incorporation of the role of functional groups and biochar porosity depending on the feedstock type and its consequent manifestation in geo-environmental and geological infrastructure. Further computational analysis is also required to establish models for analyzing properties of biochar-amended soils [72].

Acknowledgments This work was financially supported by the National Natural Science Foundation of China (grant No. 41722209).

References

1. Joseph S, Peacocke C, Lehmann J, Munroe P (2009) Developing a biochar classification and test methods. Biochar Environ Manag Sci Technol 1:107–126
2. Chen XW, Wong JTF, Chen ZT, Tang TWL, Guo HW, Leung AOW, Ng CWW, Wong MH (2018) Effects of biochar on the ecological performance of a subtropical landfill. Sci Total Environ 644:963–975
3. Wang Y, Wang H-S, Tang C-S, Gu K, Shi B (2019) Remediation of heavy-metal-contaminated soils by biochar: a review. Environ Geotech 1–14
4. White JE, Catallo WJ, Legendre BL (2011) Biomass pyrolysis kinetics: a comparative critical review with relevant agricultural residue case studies. J Anal Appl Pyrolysis 91(1):1–33
5. Rodríguez-Vila A, Selwyn-Smith H, Enunwa L, Smail I, Covelo EF, Sizmur T (2018) Predicting Cu and Zn sorption capacity of biochar from feedstock C/N ratio and pyrolysis temperature. Environ Sci Pollut Res 25(8):7730–7739
6. Troeh FR, Thompson LM (2005) Soils and soil fertility, vol 489. Blackwell New York, New York
7. Lehmann J, Joseph S (2015) Biochar for environmental management: science, technology and implementation. Earthscan, London
8. Beall FC, Eickner HW (1970) Thermal degradation of wood components: a review of the literature, vol 130. US Forest Products Laboratory, Madison
9. Barreto PLM, Pires ATN, Soldi V (2003) Thermal degradation of edible films based on milk proteins and gelatin in inert atmosphere. Polym Degrad Stab 79(1):147–152
10. Bordoloi S, Garg A, Sekharan S (2017) A review of physio-biochemical properties of natural fibers and their application in soil reinforcement. Adv Civ Eng Mater 6(1):323–359
11. Jeffery S, Verheijen FGA, van der Velde M, Bastos AC (2011) A quantitative review of the effects of biochar application to soils on crop productivity using meta-analysis. Agric Ecosyst Environ 144(1):175–187
12. Reddy KR, Yaghoubi P, Yukselen-Aksoy Y (2015) Effects of biochar amendment on geotechnical properties of landfill cover soil. Waste Manag Res 33(6):524–532
13. Sadasivam BY, Reddy KR (2015) Adsorption and transport of methane in landfill cover soil amended with waste-wood biochars. J Environ Manag 158:11–23
14. Sadasivam BY, Reddy KR (2015) Adsorption and transport of methane in biochars derived from waste wood. Waste Manag 43: 218–229
15. Feng S, Leung AK, Liu HW, Ng CWW, Zhan LT, Chen R (2019) Effects of thermal boundary condition on methane oxidation in landfill cover soil at different ambient temperatures. Sci Total Environ 692:490–502
16. Zhan L, Wu T, Feng S, Lan J, Chen Y (2020) A simple and rapid in situ method for measuring landfill gas emissions and methane oxidation rates in landfill covers. Waste Manag Res 38(5):588–593
17. Ni JJ, Chen XW, Ng CWW, Guo HW (2018) Effects of biochar on water retention and matric suction of vegetated soil. Geotech Lett 8(2):124–129. https://doi.org/10.1680/jgele.17.00180
18. Ng CWW, Ni JJ, Leung AK (2019) Effects of plant growth and spacing on soil hydrological changes: a field study. Géotechnique: 1–15
19. Wong, T.F., Wong, M.H., Ng, C.W.W., Chan, C.S., Shin, Y., Tsui, C.Y., Kim, J.J., Choy, K., Reis, R., Liu, N. (2016) A field investigation on the effects of biochar on soil aggregation in landfill final cover. paper presentation, Third International Conference on Contaminated Land, Ecological Assessment and Remediation, (CLEAR 2016), Taipei, Taiwan
20. Wong JTF, Chen Z, Ng CWW, Wong MH (2016) Gas permeability of biochar-amended clay: potential alternative landfill final cover material. Environ Sci Pollut Res 23(8):7126–7131
21. Yargicoglu EN, Reddy KR (2018) Biochar-amended soil cover for microbial methane oxidation: effect of biochar amendment ratio and cover profile. J Geotech Geoenviron Eng 144(3):4017123
22. Yargicoglu EN, Reddy KR (2017) Effects of biochar and wood pellets amendments added to landfill cover soil on microbial methane oxidation: a laboratory column study. J Environ Manag 193: 19–31
23. Yargicoglu EN, Reddy KR (2017) Microbial abundance and activity in biochar-amended landfill cover soils: evidence from large-scale column and field experiments. J Environ Eng 143(9): 4017058. https://doi.org/10.1061/(ASCE)EE.1943-7870.0001254
24. Sadasivam, B.Y., Reddy, K.R. (2015) Shear strength of waste–wood biochar and biochar–amended soil used for sustainable landfill cover systems. From Fundam. to Appl. Geotech., 745–52
25. Yargicoglu EN, Sadasivam BY, Reddy KR, Spokas K (2015) Physical and chemical characterization of waste wood derived biochars. Waste Manag 36:256–268
26. Wong JTF, Chen Z, Chen X, Ng CWW, Wong MH (2017) Soil-water retention behavior of compacted biochar-amended clay: a novel landfill final cover material. J Soils Sediments 17(3):590–598

27. Chen X-W, Wong JT-F, Ng CW-W, Wong M-H (2016) Feasibility of biochar application on a landfill final cover—a review on balancing ecology and shallow slope stability. Environ Sci Pollut Res 23(8):7111–7125
28. Xie L, Liang X, Su T-C (2018) Measurement of pressure in viewable hole erosion test. Can Geotech J 55(10):1502–1509
29. Kumar H, Ganesan SP, Bordoloi S, Sreedeep S, Lin P, Mei G, Garg A, Sarmah AK (2019) Erodibility assessment of compacted biochar amended soil for geo-environmental applications. Sci Total Environ 672:698–707. https://doi.org/10.1016/j.scitotenv.2019.03.417
30. Jyoti Bora, M., Bordoloi, S., Kumar, H., Gogoi, N., Zhu, H.-H., Sarmah, A.K., Sreeja, P., Sreedeep, S., Mei, G. (2020) Influence of biochar from animal and plant origin on the compressive strength characteristics of degraded landfill surface soils Int J Damage Mech, 1056789520925524
31. Pardo GS, Sarmah AK, Orense RP (2018) Mechanism of improvement of biochar on shear strength and liquefaction resistance of sand. Géotechnique 69(6):471–480
32. Ng CWW, Leung AK, Woon KX (2014) Effects of soil density on grass-induced suction distributions in compacted soil subjected to rainfall. Can Geotech J 51(3):311–321
33. ASTM D2166-06. (2006) Standard test method for unconfined compressive strength of cohesive soil Annu B ASTM Stand 2166
34. ASTM D4647-13. (2013) Standard test methods for identification and classification of dispersive clay soils by the pinhole test. Annu. B. ASTM Stand., Doi: https://doi.org/10.1520/D4647_D4647M-13
35. Leung AK, Garg A, Ng CWW (2015) Effects of plant roots on soil-water retention and induced suction in vegetated soil. Eng Geol 193:183–197
36. Gopal P, Bordoloi S, Ratnam R, Lin P, Cai W, Buragohain P, Garg A, Sreedeep S (2019) Investigation of infiltration rate for soil-biochar composites of water hyacinth. Acta Geophys 67(1):231–246
37. Vakili AH, Kaedi M, Mokhberi M, bin Selamat MR, Salimi M (2018) Treatment of highly dispersive clay by lignosulfonate addition and electroosmosis application. Appl Clay Sci 152:1–8
38. Sherard JL, Steele EF, Decker RS, Dunnigan LP (1976) Pinhole test for identifying dispersive soils. J Geotech Eng Div 102(1):69–85
39. Kumar H, Bordoloi S, Yamsani SK, Garg A, Sekharan S, Rakesh RR (2019) Erosion potential of compacted surface soils for multi-layered cover system. Adv Civ Eng Mater 8(1). https://doi.org/10.1520/acem20180088
40. Tian Z, Gao W, Kool D, Ren T, Horton R, Heitman JL (2018) Approaches for estimating soil water retention curves at various bulk densities with the extended van Genuchten model. Water Resour Res 54(8):5584–5601
41. Bordoloi S, Hussain R, Garg A, Sreedeep S, Zhou W-H (2017) Infiltration characteristics of natural fiber reinforced soil. Transp Geotech 12:37–44
42. Devices, D. (2013) Mini disk infiltrometer user's manual version 10
43. Astm D (2011) 2487, standard classification of soils for engineering purposes (unified soil classification system). Annu B ASTM Stand 4:206–215
44. ASTM D4318-10. (2010) Standard test method for liquid limit. Annu. B. ASTM Stand
45. ASTM D422-63. (2007) Standard test method for particle size analysis of soils. Annu. B. ASTM Stand
46. Standard test methods for specific gravity of soil solids by water pycnometer (2014). ASTM International, West Conshohocken, PA
47. ASTM D698-12. (2012) Standard test methods for laboratory compaction characteristics of soil using standard effort. Annu. B. ASTM Stand
48. Manyà JJ (2012) Pyrolysis for biochar purposes: a review to establish current knowledge gaps and research needs. Environ Sci Technol 46(15):7939–7954
49. Stuart BH, Craft L, Forbes SL, Dent BB (2005) Studies of adipocere using attenuated total reflectance infrared spectroscopy. Forensic Sci Med Pathol 1(3):197–201
50. Kinney TJ, Masiello CA, Dugan B, Hockaday WC, Dean MR, Zygourakis K, Barnes RT (2012) Hydrologic properties of biochars produced at different temperatures. Biomass Bioenergy 41:34–43
51. Gray M, Johnson MG, Dragila MI, Kleber M (2014) Water uptake in biochars: the roles of porosity and hydrophobicity. Biomass Bioenergy 61:196–205. https://doi.org/10.1016/j.biombioe.2013.12.010
52. ASTM D1762-84. (2013) Standard test method for chemical analysis of wood charcoal,. Annu. B. ASTM Stand., Doi: https://doi.org/10.1520/D1762-84R13
53. Munera-Echeverri JL, Martinsen V, Strand LT, Zivanovic V, Cornelissen G, Mulder J (2018) Cation exchange capacity of biochar: an urgent method modification. Sci Total Environ 642:190–197
54. Das O, Sarmah AK, Bhattacharyya D (2015) Structure–mechanics property relationship of waste derived biochars. Sci Total Environ 538:611–620
55. Cabanettes F, Joubert A, Chardon G, Dumas V, Rech J, Grosjean C, Dimkovski Z (2018) Topography of as built surfaces generated in metal additive manufacturing: a multi scale analysis from form to roughness. Precis Eng 52:249–265
56. Normalización, O.I. de. (2004) ISO 13322-1: 2004 (E), particle size analysis, image analysis methods. Static Image Analysis Methods. ISO
57. ISO 9278-6. (2008) Representation of results of particle size analysis–part 6: descriptive and quantitative representation of particle shape and morphology. ISO
58. Downie A, Crosky A, Munroe P (2009) Physical properties of biochar. Biochar Environ Manag Sci Technol 1
59. Zong Y, Chen D, Lu S (2014) Impact of biochars on swell–shrinkage behavior, mechanical strength, and surface cracking of clayey soil. J Plant Nutr Soil Sci 177(6):920–926. https://doi.org/10.1002/jpln.201300596
60. Zebarth BJ, Neilsen GH, Hogue E, Neilsen D (1999) Influence of organic waste amendments on selected soil physical and chemical properties. Can J Soil Sci 79(3):501–504
61. Fidel RB, Laird DA, Thompson ML, Lawrinenko M (2017) Characterization and quantification of biochar alkalinity. Chemosphere 167:367–373
62. Reddy KR, Yargicoglu EN, Yue D, Yaghoubi P (2014) Enhanced microbial methane oxidation in landfill cover soil amended with biochar. J Geotech Geoenviron Eng 140(9):4014047
63. Hanson RS, Hanson TE (1996) Methanotrophic bacteria. Microbiol Rev 60(2):439–471
64. Singh B, Singh BP, Cowie AL (2010) Characterisation and evaluation of biochars for their application as a soil amendment. Soil Res 48(7):516–525
65. Zhang TW, Cui YJ, Lamas-Lopez F, Calon N, Costa D'Aguiar S (2018) Compacted soil behaviour through changes of density, suction, and stiffness of soils with remoulding water content. Can Geotech J 55(2):182–190
66. Guo Y, Tang H, Li G, Xie D (2014) Effects of cow dung biochar amendment on adsorption and leaching of nutrient from an acid yellow soil irrigated with biogas slurry. Water Air Soil Pollut 225(1):1820
67. Markgraf W, Horn R, Peth S (2006) An approach to rheometry in soil mechanics—structural changes in bentonite, clayey and silty soils. Soil Tillage Res 91(1–2):1–14
68. Sun F, Lu S (2014) Biochars improve aggregate stability, water retention, and pore-space properties of clayey soil. J Plant Nutr Soil Sci 177(1):26–33
69. Bordoloi S, Gopal P, Boddu R, Wang Q, Cheng Y-F, Garg A, Sreedeep S (2019) Soil-biochar-water interactions: role of biochar

from Eichhornia crassipes in influencing crack propagation and suction in unsaturated soils. J Clean Prod 210:847–859. https://doi.org/10.1016/j.jclepro.2018.11.051

70. Ajayi AE, Holthusen D, Horn R (2016) Changes in microstructural behaviour and hydraulic functions of biochar amended soils. Soil Tillage Res 155:166–175. https://doi.org/10.1016/j.still.2015.08.007
71. Jeffery S, Meinders MBJ, Stoof CR, Bezemer TM, van de Voorde TFJ, Mommer L, van Groenigen JW (2015) Biochar application does not improve the soil hydrological function of a sandy soil. Geoderma 251:47–54
72. Garg A, Huang H, Kushvaha V, Madhushri P, Kamchoom V, Wani I, Koshy N, Zhu HH (2020) Mechanism of biochar soil pore–gas–water interaction: gas properties of biochar-amended sandy soil at different degrees of compaction using KNN modeling. Acta Geophysica 68(1):207–217